Anal. Chem. **2003,** *75,* 5012−5021

Resolution of Multiple ssDNA Structures in Free Solution Electrophoresis

Eve F. Fabrizio, Ali Nadim, and James D. Sterling*

Keck Graduate Institute of Applied Life Sciences, Claremont, California 91711

By using high concentrations of buffer, electroosmotic flow within uncoated channels of a microfluidic chip was minimized, allowing the free solution electrophoretic separation of DNA. More importantly, because of the ability to efficiently dissipate heat within these channels, field strengths as high as 600 V/cm could be applied with minimal Joule heating (< 2 °C). As a result of the higher field strengths, separations within an 8-cm-long channel were achieved within a few minutes. However, when the electrophoretic separation of single-stranded DNA (ssDNA) less than 22 bases in length was performed, containing the fluorophore Texas Red as an end label, more than the expected single peak was observed at this high electric field. On the other hand, the free solution electrophoresis of a double-stranded DNA (dsDNA) consisting of a random sequence did exhibit the expected single peak. The appearance of these multiple peaks for ssDNA is shown to be dependent upon the base content and sequence of the ssDNA as well as on the chemical structure of the fluorophore used to tag the DNA for detection. Specifically, the peaks can be attributed to different secondary structures that result either from hydrophobic interactions between the DNA bases and an uncharged fluorescent dye or from G-quadruplexes within guanine-rich strands.

Electrophoretic mobility of a charged molecule under the influence of an applied electric field is proportional to the ratio of total charge to drag coefficient if the molecule is small compared to the Debye length of the solution.[1] For longer strands of DNA or any other polyelectrolyte, this ratio is constant and independent of fragment length or size, making it difficult to separate DNA in free solution. To differentiate between different lengths of DNA, electrophoresis is commonly performed in the presence of a sieving matrix, which alters the mobility based on fragment size. In gel electrophoresis, the sieving matrix is a cross-linked polymer network, whereas in capillary electrophoresis, a linear polymer is added to the buffer. The addition of sieving matrixes to the buffer, however, makes it difficult to interface the output of the capillary to a second analytical system such as a mass spectrometer or to do additional manipulation or studies on the sample: for example, binding studies between DNA and proteins. An alternative to adding sieving matrix is to lithographically design constrictions within the channels that are on the order of molecular dimensions, but like gel electrophoresis, such systems primarily work for longer strands of DNA.[2−8]

Another strategy devised to eliminate the need for sieving matrixes is to alter the drag coefficient of each polyelectrolyte strand without changing the total charge.[9] One popular means of achieving this type of separation is to attach a large mass, such as streptavidin, to one end of the polyelectrolyte or DNA.[10−17] This technique, which is called end-labeled free solution electrophoresis or ELFSE, has been shown to be quite useful for a wide range of DNA fragments. Detailed discussions of the effects on ELSFE of the size of the end label, the contour and persistence lengths of the DNA, the Debye length, and the ionic strength of the buffer, both with and without sieving interactions, have been provided by Desruisseaux et al.[18,19] Additional electrophoretic studies by Stellwagen et al., on the other hand, have indicated that such labeling may not be necessary for DNA fragments that are less than 400 bp in length.[20−22] Specifically, by performing the free solution capillary electrophoresis (FSCE) of small DNA fragments, the electrophoretic mobility was discovered to decrease with strand length. Thus, FSCE can be utilized to identify or separate

* To whom correspondence should be addressed. Phone: 909-607-9253. E-mail: Jim_Sterling@kgi.edu.

(1) For a review of the electrophoresis of DNA, see: Viovy, J.-L. *Rev. Mod. Phys.* **2000**, *72*, 813−872.
(2) Wolkmuth, W. D.; Austin, R. H. *Nature* **1992**, *358*, 600−602. Han, J.; Craighead, J. C. *Science* **2002**, *288*, 1026−1029.
(3) Austin, R. H.; Volkmuth, W. D. *Analysis* **1993**, *21*, 235−238.
(4) Duke, T. A. J.; Austin, R. H. *Phys. Rev. Lett.* **1998**, *80*, 1552−1555.
(5) Han, J.; Craighead, J. C. *Science* **2000**, *288*, 1026−1029.
(6) Han, J.; Craighead, H. G. *Anal. Chem.* **2002**, *74*, 394−401.
(7) Turner, S. W. P.; Cabodi, M.; Craighead, H. G. *Phys. Rev. Lett.* **2002**, *88*, 128103.
(8) Cabodi, M.; Turner, S. W. P.; Craighead, H. G. *Anal. Chem.* **2002**, *74*, 5169−5174.
(9) For review, see: Righetti, P. G.; Gelfi, C. *J. Biochem. Biophys. Methods* **1999**, *41*, 75−90.
(10) Reference 1, p 860.
(11) Noolandi, J. *Electrophoresis* **1992**, *13*, 394−395.
(12) Noolandi, J. *Electrophoresis* **1993**, *14*, 680−681.
(13) Mayer, P.; Slater, G. W.; Drouin, G. *Anal. Chem.* **1994**, *66*, 1777.
(14) Volkel, A. R.; Noolandi, J. *Macromolecules* **1995**, *28*, 8182−8189.
(15) Heller, C.; Slater, G. W.; Mayer, P.; Dovichi, N.; Pinto, D.; Viovy, J.-L.; Drouin, G. *J. Chromatogr., A* **1998**, *806*, 113−121.
(16) Hoagland, D. A.; Arvanitidou, E.; Welch, C. *Macromolecules* **1999**, *32*, 6180−6190.
(17) Ren, H.; Karger, A. E.; Oaks, F.; Menchen, S.; Slater, G. W.; Drouin, G. *Electrophoresis* **1999**, *20*, 2501−2509.
(18) Desruisseaux, C.; Long, D.; Drouin, G.; Slater, G. W. *Macromolecules* **2001**, *34*, 44−52.
(19) Desruisseaux, C.; Drouin, G.; Slater, G. W. *Macromolecules* **2001**, *34*, 5280−5286.
(20) Stellwagen, N. C.; Gelfi, C.; Righetti, P. G. *Biopolymers* **1997**, *42*, 687−703.
(21) Mohanty, U.; Stellwagen, N. C. *Biopolymers* **1999**, *49*, 209−214.
(22) Stellwagen, E.; Stellwagen, N. C. *Electrophoresis* **2002**, *23*, 2794−2803.

10.1021/ac034326c CCC: $25.00
Published on Web 08/22/2003

oligonucleotides that are less than 20−30 bases in length that are of increasing interest for genetic analysis including agriculture, forensics, pathogen detection, and pharmacogenomics.

While capillaries are the preferred choice for the electrophoretic separation of DNA, there are a number of practical advantages to utilizing microfluidic chips in lieu of standard capillaries. First is size. The chips used in our experiments are only 1.6 cm in width and 9.5 cm in length. With appropriate power supplies, detection system, and electronics, development of a portable electrophoresis system is feasible. Also, because of size, the buffer and sample volumes are considerably smaller. Second, with chips now being manufactured from polymeric materials such as poly(dimethylsiloxane), chip-based electrophoresis systems have the potential to be less expensive than the standard capillary systems. Finally, since the channels on a microfluidic chip can be manufactured with a variety of geometric dimensions, the surface-to-volume ratio can be maximized, resulting in more efficient heat dissipation and less Joule heating. As a result, a high electric field can be applied resulting in faster electrophoretic velocities, which facilitate separations on the order of minutes instead of hours.

Another advantage to applying high fields is enhanced resolution. The following scaling argument indicates the need for high field strengths in order to be able to resolve two species with very similar mobilities (and diffusivities) in a capillary electrophoresis system of finite length. Denote the velocities of the two species by u_1 and u_2 and their difference by Δu. Since the mobilities are assumed to be quite similar, $u_1 \approx u_2 \approx U$ and $\Delta u \ll U$. Here, U denotes the order of magnitude of the two migration velocities. Note that both U and Δu are proportional to the electric field strength E. In a capillary of length L, the typical time available for the experiment is given by $t_{exp} = L/U$, which is the time it takes for the bands to travel the length of the capillary. After such a time interval, the expected spatial distance between the two peaks corresponding to the two species is given by $l_P = \Delta u t_{exp} = \Delta u L/U$. If we characterize the molecular diffusivities of the two species by D, during that same time interval, the typical diffusion length for each species is given by $l_D = (2Dt_{exp})^{1/2} = (2DL/U)^{1/2}$. Note that our assumption that D is independent of the electric field is not valid in gel electrophoresis but is valid under free solution conditions considered here.[23,24] Resolution, R_s, is defined as $R_s \equiv l_P/(4l_D)$ such that in order to provide a high value of resolution for the two bands, the diffusion length must be much less than the peak separation, i.e., $l_D \ll l_P$.[25] Using our estimates for these two lengths, this definition implies that the length of the separation channel must satisfy the relationship $L = 32R_s^2UD/(\Delta u)^2$. Since both U and Δu are directly proportional to E, we find that the separation length required to obtain a desired resolution scales as the reciprocal of the electric field strength; i.e., the higher the field, the shorter the capillary channel needed for the resolution. In a channel of finite length, if the mobilities of the two species are very close, unless the field is strong enough to pull apart the peaks in a short enough time (over which the diffusion length remains small compared to the peak separation), the two species cannot be resolved.

The work presented here evaluates the ability to electrophoretically separate single-stranded DNA (ssDNA) and double-stranded DNA (dsDNA) less than 100 bp in length using high field strengths on a microfluidic chip containing a separation channel that is 8 cm in length and has a cross section with a semicircular/rectangular shape: width of 50 μm and depth of 20 μm. Additionally, instead of coating the channels to minimize EOF, we chose to minimize EOF by increasing the concentration of the buffer. Since laser-induced fluorescence is used for detection, the DNA fragments were labeled by attaching a fluorescent dye to either the 5′ or 3′ end of each strand. Because the size of these fluorescent labels is on the order of two to three deoxyribonucleotides, we expect the electrophoretic mobility to be influenced by changes in the frictional drag, especially with shorter length DNA strands as in ELFSE. Therefore, these results provide insight into how the DNA structure and corresponding end label impact electrophoretic migration in free solution.

EXPERIMENTAL SECTION

Materials. The buffers used in this study were 10×, 5×, 2.5×, 1×, 0.5×, and 0.1× Tris−borate−sodium EDTA (TBE) at pH 8.3. The 10× TBE (890 mM Tris−borate and 20 mM EDTA) was used as received (Fisher Scientific). The rest of the concentrations were prepared by diluting 10× TBE with an appropriate amount of Milli-Q water (Millipore). The 10× TBE at pH 7 was prepared by titrating 10× TBE at pH 8.3 with concentrated HCl (Fisher Scientific). The pH during the titration was measured using a pH meter and probe (Fisher Scientific). In solutions where urea was added to minimize hydrogen-bonding interactions, an appropriate amount of urea (Fisher Scientific) was weighed and dissolved into the desired buffer. The 22.5× Tris−acetate−sodium EDTA (TAE) was prepared by diluting 4.5 mL of 25× TAE (900 mM Tris−acetate and 22.5 mM EDTA; Fisher Scientific) with 0.5 mL of Milli-Q water (Millipore). Immediately prior to use, each buffer solution was filtered with a GHP Acrodisc 25-mm syringe filter with a 0.22-μm GHP membrane (Pall Gelman Laboratory). The uncharged or zwitterionic dye used to measure electroosmotic flow was Rhodamine B (Sigma-Aldrich). The dye stock solution consisted of a 1 mM solution in a 1:1 methanol/water solution to facilitate dissolution of the uncharged dye.

The following single-stranded DNA oligomers of HPLC (RP) grade (Midland Certified Reagent Co., Midland, TX) were also used as received: 5′-TGGATCAGCAAGCAGGAGTAT-3′ (21 mer), 5′-ATCAGCAAGCAGGAG-3′ (15 mer), 5′-AGCAAGCAG-3′ (9 mer), $d(A)_{15}$, $d(T)_{15}$, $d(C)_{15}$, and $d(G)_{15}$. All oligomers were labeled with Texas Red (excitation 580 nm, emission 600 nm; Molecular Probes, Inc.) using either a C6 or C7 linker with the label on the 5′ end of the oligomer except for $d(A)_{15}$, which, to facilitate hybridization with the labeled $d(T)_{15}$, was labeled on the 3′ end. Additionally, $d(A)_{15}$ and $d(G)_{15}$ were also labeled with Cy3 (excitation 548 nm, emission 562 nm; Amersham Biosciences). In addition to these labeled oligomers, an unlabeled $d(C)_{15}$ and a complement to the above labeled random-sequenced 15 mer were synthesized for hybridization to their corresponding labeled complements.

Electrophoresis. Capillary electrophoresis was performed using the Microfluidic Tool Kit from Micralyne, Inc. (Edmonton,

(23) Meistermann, L.; Tinland, B. *Phys. Rev. E* **1998**, *58*, 4801−4806.
(24) Nkodo, A. E.; Garnier, J. M.; Tinland, B.; Ren, H.; Desruisseaux, C.; McCormick, L. C.; Drouin, G.; Slater, G. W. *Electrophoresis* **2001**, *22*, 2424−2432.
(25) Giddings, J. C. *Unified Separation Science*; John Wiley and Sons: New York, 1991; pp 92−105.

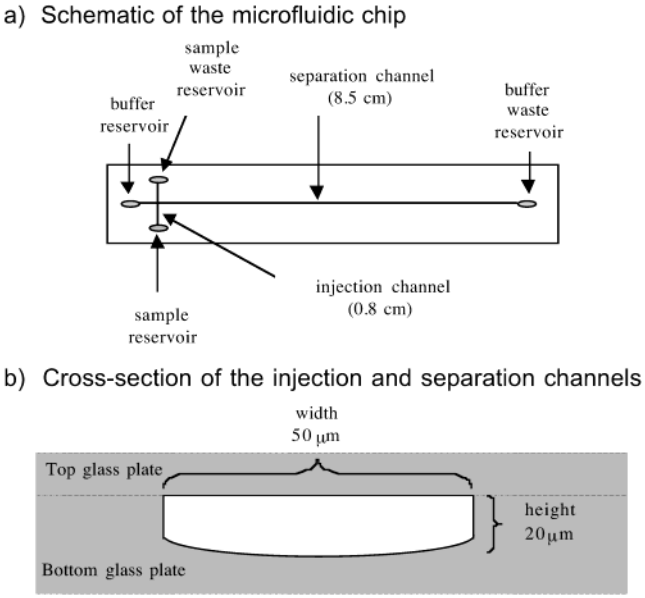

Figure 1. Schematic of the microfluidic chip (a) and of a cross section of the channels (b). (The actual thickness of the top and bottom plates is 1.1 mm and is not drawn to scale in this figure.)

Alberta, Canada). This system consists of two 5-kV power supplies that supply a potential difference across the injection and separation channels of a microfluidic chip. The optical system for obtaining the fluorescence signal within the channels contains an *x*, *y*, and *z* positioner (Newport Optics) that allows one to focus a 40× objective (NA 0.55) anywhere along the injection or separation channels. This objective sends the image including the fluorescence to either an eyepiece for visual inspection or a photomultiplier tube (Hamamatsu) for emission detection. The excitation light source is an Nd:YAG (532 nm) diode pumped solid-state laser. To facilitate the detection of a wide range of fluorophore emission wavelengths, a 560-nm long-pass filter (12.7 mm in diameter; Coherent) was employed. The system was controlled using Labview (National Instruments, Austin, TX). A more detailed description and schematic of the system are provided in a previously published reference.[26]

The glass microfluidic chip that was used in these experiments was also obtained from Micralyne, Inc. The chip contained a simple cross format with channels consisting of a semicircular cross section with a 50-μm width and a 20-μm depth. A detailed schematic of the chip and channel is provided in Figure 1.

Between each series of experiments, the chip was cleaned using the following procedure. All reservoirs and channels were flushed three times with 1.5 M HNO_3 (Acros Organics), then 1.0 M NaOH (Fisher Scientific), and then filtered Milli-Q water by filling the buffer, sample, and sample waste reservoirs with each cleaning solution and by applying suction to the buffer waste reservoir. The channels were then flushed with the electrophoretic buffer for each experiment using the same method. When not in use, the chip was stored in Milli-Q water to prevent the channels from drying out, which could result in crystallization of residual salts.

To properly evaluate the amount of Joule heating in the separation channel during electrophoresis, an ammeter (Multitec 320; Extech Instruments) was placed in series between the power supply and one of the electrodes going to the separation channel on the microfluidic chip. (Safety Note: Because of the high voltages applied during the experiment, the ammeter and any exposed leads were placed within a Plexiglas box to eliminate any chance of human contact.) In addition to measuring the current during electrophoresis, the temperature of the surface of the chip directly under the separation channel was measured using a subminiature connector with a spool cap T-type thermocouple insulated with Teflon (Omega Engineering, Inc., Stamford, CT). The thermocouple was placed in contact with the glass by using thermally conductive epoxy (Silver Conductive Epoxy; M.E. Taylor Engineering, Inc., Brookeville, MD). The thermocouple was read using a Cole Palmer Digi-Sense temperature controller (Cole Palmer, Vernon Hills, IL).

Electroosmotic flow (EOF) or velocity was determined by measuring the retention time of a zwitterionic or uncharged fluorescent dye, Rhodamine B, within a given distance along the separation channel on the chip. The sample reservoir was filled with 3.4 μL of buffer containing 10 μM Rhodamine B while the other three wells were filled with 3.4 μL of the buffer. Injection of a dye plug into the separation channel was accomplished by electroosmotically pumping the dye from the positively biased sample reservoir to the grounded sample waste reservoir by applying a field of 2500 V cm^{-1} across the injection channel for 20 s. This was followed by electroosmotically pumping the dye from the positively biased buffer reservoir to the grounded buffer waste by applying a field of 588 V cm^{-1} across the separation channel. To minimize any pressure-driven flows due to uneven volumes in the reservoirs as a result of evaporation and EOF, the reservoirs were emptied and refilled prior to the start of each measurement.[26] An average electroosmotic velocity was determined by measurements obtained prior to, during, and immediately after any given experiment. All measurements showed a <3% variance in the velocity, demonstrating the consistency and reproducibility of using uncoated channels.

For the free solution electrophoresis of both ssDNA and dsDNA, a procedure similar to the one above was used. First, DNA stock solutions were prepared by dissolving the solid oligomer in Milli-Q water so that each had a final concentration of approximately 100−200 μM. Any unused portion of the stock solution was stored in a −20 °C freezer. Sample solutions were then made by dissolving 1 μL of the stock solution into 19 μL of the electrophoretic buffer to minimize any dilution of the buffer (final concentration after dilution, 860 mM Tris−borate EDTA). For free solution electrophoresis of dsDNA, 1 μL of each of the complement strands was added to 5 μL of the electrophoretic buffer. This solution was allowed to sit at room temperature for 30 min to hybridize prior to adding an additional 15 μL of buffer. For these measurements, 3.4 μL of each of the DNA solutions was placed into the sample reservoir and 3.4 μL of buffer was placed in the other three reservoirs. The DNA was injected into the separation channel by electrophoretically migrating the DNA from the grounded sample reservoir to the positively biased sample waste reservoir by applying a field of 2500 V cm^{-1} across the injection channel for 20 s. Electrophoresis was accomplished by applying an electric field of 588 V cm^{-1}, unless otherwise stated, across the separation channel. Note, that the direction of these

(26) Crabtree, H. J.; Cheong, E. C. S.; Tilroe, D. A.; Backhouse, C. J. *Anal. Chem.* **2001**, *73*, 4079−4086.

fields is opposite to those used for electroosmotically pumping the neutral dye. The separation distance or length, which is the distance the detector was positioned from the injection channel or cross, is provided on each electrophorogram. The electrophoretic velocity (U_{EP}) for each of the oligomers was determined by adding the electroosmotic velocity (U_{EOF}) measured using the neutral dye to the total or apparent velocity ($U_{app.}$) measured for the oligomers in the electrophorogram;

$$U_{EP} = U_{app.} + U_{EOF} \quad (1)$$

The field strength (E) and electrophoretic velocity were then used to calculate electrophoretic mobility (μ_{EP}):

$$\mu_{EP} = U_{EP}/E \quad (2)$$

All values are an average of three or more runs.

Melting Temperatures for dsDNA. Melting curves of dsDNA were obtained using a Roche Light Cycler (Roche Applied Science, Indianapolis, IN). Samples were prepared by mixing together 15 μL of the complementary ssDNA strands using the same stock solutions prepared for electrophoresis with 200 μL of SYBR Green I diluted to 1:1000 with 1× TE (1:10 000; Sigma-Aldrich) and 1000 μL of 10× TBE. Each dsDNA sample (A−T and G−C) was then placed in the instrument and the gain adjusted to obtain maximum fluorescence signal. The fluorescence signal was then recorded as the temperature was ramped from room temperature (23 °C) to 100 °C at a rate of 0.1 °C s^{-1}. The melting temperatures (T_m) were estimated from the midway point between the maximum and minimum fluorescence in the curve. Experimental values were also compared to theoretical values obtained from OligoAnalyzer 3.0 from Integrated DNA Technologies (www.idtdna.com; Coralville, IN). Experimental values showed good agreement with theoretical (±5.0 °C).

RESULTS AND DISCUSSION

Minimization of EOF and the Free Solution Capillary Electrophoresis of ssDNA. When an external potential field is applied to a glass channel with an internal negative surface charge, electroosmotic flows develop. As previous studies have shown, the free solution electrophoretic separation of short DNA fragments (<100 bp) can only be achieved by utilizing a method that keeps the electroosmotic velocity less than the electrophoretic velocity of the charged DNA fragments being analyzed. The electroosmotic flow or velocity is expressed by the Helmholtz−Smoluchowski equation:

$$U_{EOF} = (\epsilon\epsilon_o\zeta/\eta)E \quad (3)$$

where ϵ is the dielectric constant of the solution in the capillary (water, $\epsilon = 80$), ϵ_o is the permittivity in a vacuum ($\epsilon_o = 8.85 \times 10^{-12}$ C^2 N^{-1} m^{-2})), ζ is the potential at the shear plane or the ζ potential, and η is the viscosity of the solution in the capillary. Using the Debye−Hückel approximation, the ζ potential can be related to the surface charge (σ) by

$$\zeta = \sigma/\epsilon\epsilon_o\kappa \quad (4)$$

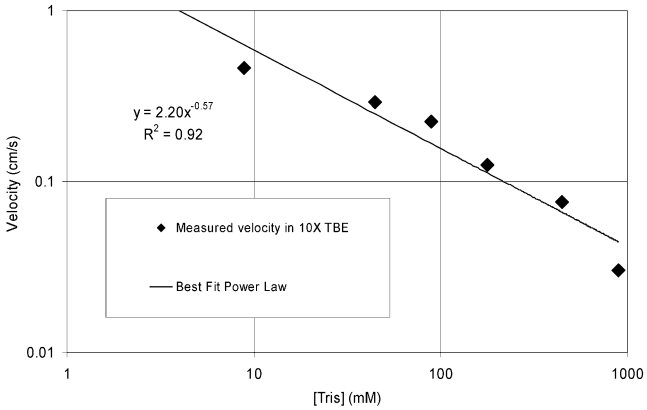

Figure 2. Decrease in the electroosmotic velocity with increasing concentration of TBE along with the predicted relative change in velocity based on change in the double-layer thickness with ionic strength.

where κ is the Debye−Hückel parameter given by

$$\kappa = \{I(2F^2/\epsilon\epsilon_o RT)\}^{0.5} \quad (5)$$

where I is the ionic strength of the solution ($I = {}^1/_2 \sum z_j^2 c_j$), F is the Faraday constant (96 485 C mol^{-1}), R is the universal gas constant (8.31 J K^{-1} mol^{-1}), and T is the absolute temperature (K). The inverse of κ is the charge screening length or the Debye length.

The conventional way of minimizing EOF is by coating the capillary walls with a neutral modifier such as *N*-acryloylaminopropanol, which decreases the charge at the surface. One disadvantage to precoating the internal walls of the capillary is that surface charge and in turn EOF can vary with the amount of coverage prior to and during a separation. Even though this variability may not affect the electrophoretic separation of species with high electrophoretic mobilities, it can significantly affect the separation of species that have lower electrophoretic mobilities such as small DNA fragments. We therefore took a different approach to decreasing EOF; decreasing the ζ potential or Debye length by increasing the ionic strength of the buffer.[27] Figure 2 shows the effect of increasing concentration of buffer (TBE) on the electroosmotic velocity of an uncharged fluorescent dye in the channels of our microchip. In addition, the best-fit power law shows a decrease corresponding to $I^{-0.57}$, which is close to the $I^{-0.5}$ behavior expected from the equations above.[27]

Based on the measured electroosmotic velocity of 0.03 cm s^{-1} at the highest concentration of TBE and field strength of 588 V cm^{-1} (5000 V/8.5 cm), the electroosmotic mobility (μ_{EOF}) is 0.5 × 10^{-4} cm^2 V^{-1} s^{-1}. This mobility is lower than the measured free solution electrophoretic mobilities (μ_{EP}) of DNA, which range from 2 × 10^{-4} to 4 × 10^{-4} cm^2 V^{-1} s^{-1}.[20−22,24] Since, in the electrophoresis of DNA, the electroosmotic flow opposes the electrophoretic migration, this difference in mobility should permit the separation of small fragments (<100 bp) in free solution without having to coat the inner walls of the capillary or channel. However, use of an increased buffer concentration also results in

(27) Thormann, W.; Zhang, C.-X.; Caslavska, J.; Gebauer, P.; Mosher, R. A. *Anal. Chem.* **1998**, *70*, 549−562.

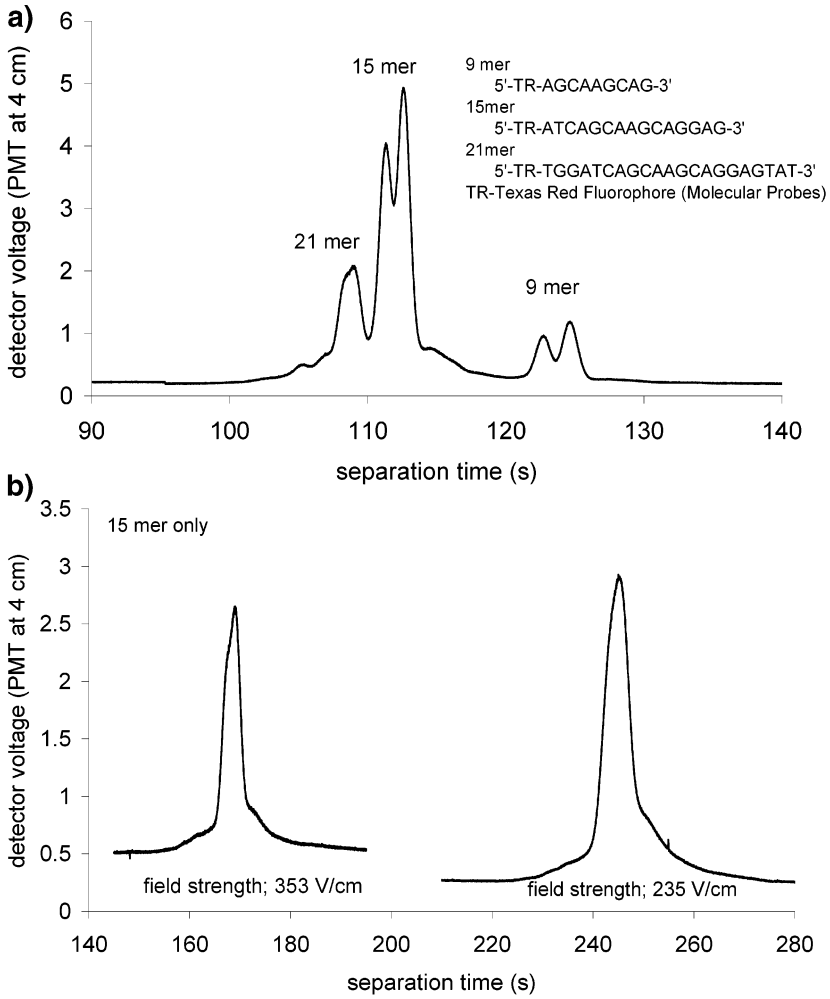

Figure 3. Free solution electrophoresis of fluorescently labeled single-stranded DNA with strand lengths of 21, 15, and 9 bases (a) at a field strength of 588 V cm^{-1} and (b) of only the 15 mer at field strengths of 353 and 235 V cm^{-1}.

a smaller Debye length that, if comparable to the size of the molecule, can lower electrophoretic mobility and increase diffusion, both of which adversely affect resolution.[16,24]

In our first attempt to separate different lengths of ssDNA, a mixture of Texas Red-labeled (5′ end) oligomers consisting of a 21 mer (5′-TGGATCAGCAAGCAGGAGTAT-3′), a 15 mer (5′-ATCAGCAAGCAGGAG-3′), and a 9 mer (5′-AGCAAGCAG-3′) was injected and separated using a field strength of 588 V cm^{-1} (5000 V/8.5 cm). As Figure 3a shows, we were able to separate these three different fragments within 2.5 min and at a separation length of 4 cm.

The retention times, which are approximately 109 s for the 21 mer, 112 s for the 15 mer, and 124 s for the 9 mer, are consistent with the trend observed in previous experiments using free solution capillary electrophoresis where electrophoretic mobility increased with increasing base length.[11−22]

One feature that is observed in our separation but not observed in previous experiments is the presence of two peaks for each of the three oligomers. Figure 3b shows the effect of lowering the field on the electrophoresis of only the 15 mer. As expected, the peaks merge into a single peak as the field strength is lowered to 235 V cm^{-1} (2000 V/8.5 cm). Thus, the ability to resolve multiple peaks for the free solution electrophoresis of the ssDNA oligomers appears to be due to the higher applied field across the channel. One unanswered question that needs to be addressed is what is the source of the multiple peaks. Is the high field causing a chemical reaction such as depurination to occur in the channel resulting in slightly different mobilities for a portion of the oligomer in solution? Are pressure-driven flows that are established in the channel during injection and separation resulting in band anomalies during the separation? Or, is the high field, as predicted, allowing us to resolve different charge-to-size components or secondary structures? The remainder of this paper will focus on determining which of these factors contributes to the formation of multiple peaks for each of the single-stranded oligomers.

Degradation of DNA by High Separation Voltages. As previously mentioned, the fields used in our experiments are approximately 3−6 times higher than those used in the free solution electrophoresis of DNA using capillaries. Hence, the most obvious explanation for the multiple peaks is that the large electric field applied across the channel is damaging the DNA. Since the oligonucleotides migrate from the ground electrode in the buffer reservoir to the positively biased electrode in the buffer waste reservoir, one might expect the damage, if any, to occur as the DNA approaches the large voltage at the positive electrode. Figure 4a shows the electrophoresis of the 15 mer as a function of distance along the separation channel.

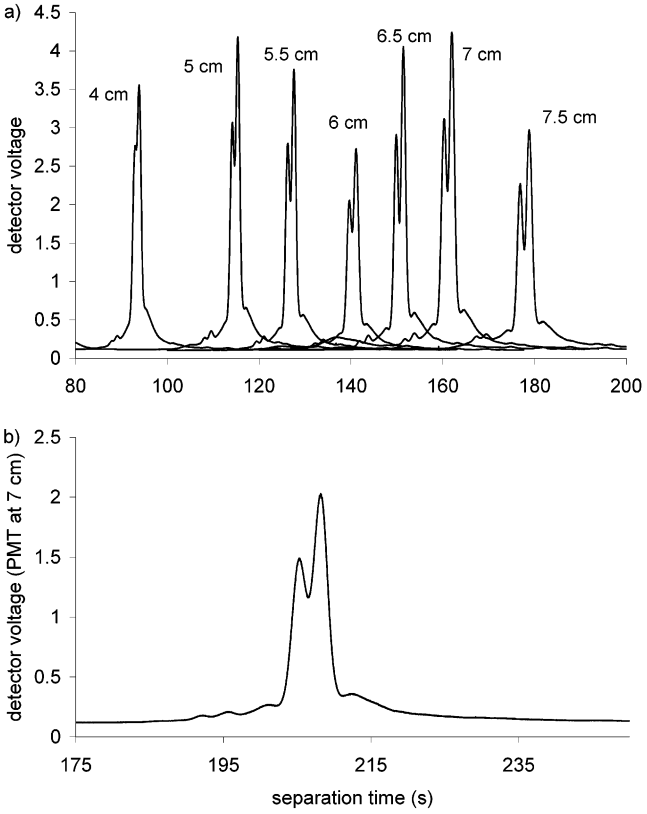

Figure 4. Free solution electrophoresis of the fluorescently labeled 15 mer: (a) peak splitting and areas as a function of channel length or separation distance and (b) after a pressure-formed plug.

A comparison of the relative area of the first and second peaks at distances greater than 5 cm indicated no change in relative peaks areas: ~40% for the first peak and ~60% for the second. Additionally, the magnitude of the time interval between the two peaks increases linearly with time or distance traveled and extrapolates to zero at the point of injection. This observation suggests that two species are present in the injection plug. Therefore, one other possibility is that the degradation may actually be occurring during the electrokinetic injection. With an injection voltage of 2000 V and an injection channel length of 0.8 cm, the oligomers are actually exposed to a field strength of 2500 V cm^{-1} over a time period of 20 s. To determine whether injection is damaging the DNA, we performed a series of plug formations in which the DNA sample was loaded into the injection channel using pressure-driven flow instead of electrokinetic flow. Figure 4b shows the electrophoresis of the 15 mer after a pressure-formed plug. Even with the elimination of the exposure of the ssDNA to a field of 2500 V cm^{-1}, two peaks with the same relative peak areas are still present. These experiments strongly suggest that the high field strength is not degrading or damaging the DNA and that the sample actually contains molecular structures with slightly different mobilities.

Chemical Reactions or Interactions Affecting Mobilities. One such interaction that could lead to multiple structures with different mobilities is the complexation of the buffer anion, borate, to the DNA strands. Previous studies by Stellwagen et al. have shown that the electrophoretic mobility of DNA increases in the presence of borate as a result of this anion complexing to DNA.[28,29] If the number of borate ions binding to any given strand varies, then fragments with different charges and in turn different mobilities could exist. This hypothesis, however, was proven incorrect by performing the electrophoresis of the 15 mer in 22.5× Tris−acetate−sodium EDTA (890 mM Tris acetate and 20 mM sodium EDTA), which is equal to the molar concentration of 10× TBE. The resulting electrophorogram is shown in Figure 5a. While the electrophoretic velocity in TAE was slower due to a greater electroosmotic flow (U_{EOF} = 0.048 cm s^{-1}), exchanging acetate ions for borate ions in the buffer did not affect either the electrophoretic mobility or the presence of the two bands.

Another source of multiple mobilities could be the presence of different ionization states that result from protonated (positively charged) and deprotonated (neutral) endocyclic amines on the bases, thymine and guanine, whose pK_a values (~9) are close to the pH of the TBE buffer (8.3). To test this hypothesis, the electrophoresis of the 15 mer was performed in 10× TBE at a pH of 7 (instead of a pH of 8.3) and the results are shown in Figure 5b. While the electrophoretic mobility of the two bands decreased (~7%) in the lower pH buffer, as would be expected due to the decrease in overall negative charge of the oligomer upon protonation of the endocyclic amines, the splitting and relative peak areas remained unchanged, eliminating ionization as the main source of this effect.

To determine whether the difference in the peak mobilities can be attributed to a difference in charge, the equation[1]

$$\mu_{EP} = q/6\pi\eta R_h \qquad (6)$$

where q is the total charge of the molecule, η is the viscosity of the buffer (0.931 × 10^{-3} N s m^{-2}; value for water at room temperature), and R_h is the hydrodynamic radius, was used to estimate the charge difference for the two peaks observed in the electrophoresis of the 15 mer in 10× TBE at pH 8.3. If we assume that the fastest peak, which has an electrophoretic mobility of 1.04 × 10^{-4} cm^2 V^{-1} s^{-1}, has the higher negative charge of −14, then $6\pi\eta R_h$ is 2.16 × 10^{-10} C V s m^{-2}. Substituting this value into eq 6 and using the measured mobility of the slower peak, 1.02 × 10^{-4} cm^2 V^{-1} s^{-1}, a charge (q) of −13.7 was calculated. The difference of only 0.3 could be attributed to charge screening of a full charge. However, the fact that the relative peak areas do not change with pH and the absence of peak splitting when the Texas Red is replaced by Cy3 (discussed later) strongly suggest that there is little effective charge difference but that there exist different structures having different hydrodynamic radii, R_h.

Since all three ssDNA oligomers contain a number of adenine (A) and guanine (G) bases, depurination, which is the cleavage of purine bases from the sugar backbone, is one means by which hydrodynamic radius and mobility can change. Although depurination occurs at a relatively slow rate at room temperature in neutral to basic solutions, decreasing the pH of the solution, increasing the temperature, or both has been shown to catalyze the rate of this reaction.[30,31] Since the concentration of buffer in our separations is high, any Joule heating within the channels

(28) Stellwagen, N. C.; Gelfi, C.; Righetti, P. G. *Biopolymers* **2000**, *54*, 137−142.
(29) Stellwagen, N. C.; Bossi, A.; Gelfi, C.; Righetti, P. G. *Anal. Biochem.* **2000**, *287*, 167−175.

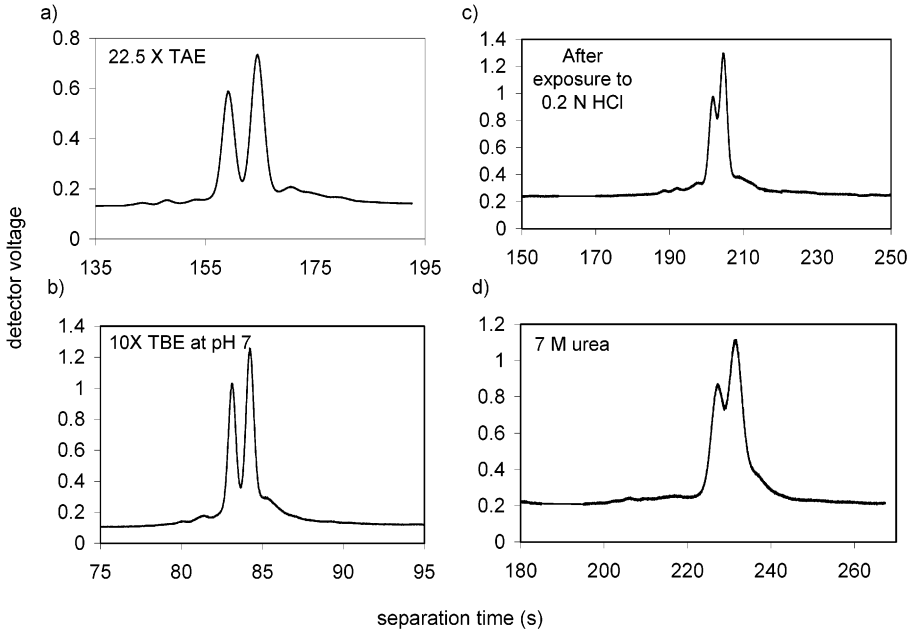

Figure 5. Free solution electrophoresis of the fluorescently labeled 15 mer in (a) 22.5× TAE, (b) 10× TBE at pH 7, (c) 10× TBE at pH 8.3 after the oligomer was exposed to 0.2 N HCl for 20 min, and in (d) 10× TBE at pH 8.3 containing 7 M urea, a hydrogen-bonding disrupter.

Table 1. Average Free Solution Electrophoretic Mobilities ($n = 3$) for ssDNA and dsDNA Fragments

	electrophoretic mobility ($\mu_{EP} \times 10^{-4}$; cm^2 V^{-1} s^{-1}) for oligomers studied							
	$d(A)_{15}$	$d(T)_{15}$	$d(G)_{15}$	$d(C)_{15}$	$d(X^*)_{15}$[a]	$ds(A-T)_{15}$	$ds(G-C)_{15}$	$ds(X^*)_{15}$[a]
peak 1	1.04	1.03	1.05	1.08	1.04	1.16	1.19	1.14
peak 2	1.02	1.00		1.05	1.03			

[a] X* indicates random sequence.

may increase the rate and amount of depurination in each oligomer. To evaluate the effect of depurination on electrophoretic mobility, the 15 mer was exposed to 0.2 N HCl for 20 min prior to electrophoresis. The resulting electrophorogram is shown in Figure 5c. When compared to the previous electrophoretic results, there is no change in the peak splitting or relative peak areas for this oligomer, suggesting no correlation between the observed splitting and depurination.

Finally, we examined the possibility of different secondary structures resulting from intra- and interstrand hydrogen bonding. Even though none of the ssDNA strands contain sequences that are self-complementary, non-Watson and Crick hydrogen bonding could lead to such interactions. These structural changes could easily alter the hydrodynamic radius and lead to slightly different mobilities. Figure 5d shows the electrophoresis of the 15 mer in the presence of 7 M urea, a denaturant or hydrogen bond disruptor. When compared to all the previous measurements, we see that the addition of urea did not alter the relative appearance of the peaks; however, the retention time for the 15 mer does increase. After taking into consideration the EOF ($U_{EOF} = 3.0 \times 10^{-2}$ cm s^{-1}) in this buffer, the median electrophoretic mobility for both peaks dropped from 1.1×10^{-4} to 0.85×10^{-4} cm^2 V^{-1} s^{-1} in the presence of the urea, likely a result of increased solution viscosity. Thus, intrastrand and interstrand hydrogen bonding, which could result in secondary structures with different frictional drag coefficients, is not contributing to the observed peak splitting.

Further confirmation that the peak splitting is associated with molecular conformations with different electrophoretic mobility was obtained by reversing the polarity of the electrode potentials several times during the course of a single run. The results, provided in the Supporting Information, conclusively show that the peak splitting is not associated with pressure-induced flows or other hydrodynamically induced dispersion.

DNA Base Sequence Effects. In an attempt to gain a better understanding of the field-based band splitting for ssDNA, we evaluated the impact of sequence on the free solution electrophoresis of ssDNA by analyzing oligomers that contained a single base. To be consistent with the above measurements, only strands containing 15 bases (or 15 mers) were studied. Panels a and b of Figure 6 show the electrophoresis of $d(A)_{15}$ and of $d(T)_{15}$, respectively, at a field strength of 588 V cm^{-1}.

From the average retention time of three runs and the measured EOF, the average electrophoretic mobilities for the corresponding peaks of each oligomer were determined and are provided in Table 1.

While previously reported values for the electrophoretic mobility of ssDNA range from 2.8 to 3.4×10^{-4} cm^2 V^{-1} s^{-1}, our values are somewhat lower due to the increase in frictional drag from the fluorescent tag as well as from the decrease in mobility with high ionic strength.[14,16,20,21,22,24] As with the random sequence,

(30) Greer, S.; Zamenhof, S. *J. Mol. Biol.* **1962**, *4*, 123−141.
(31) Lindahl, T.; Nyberg, B. *Biochemistry* **1972**, *11*, 3610−3618.

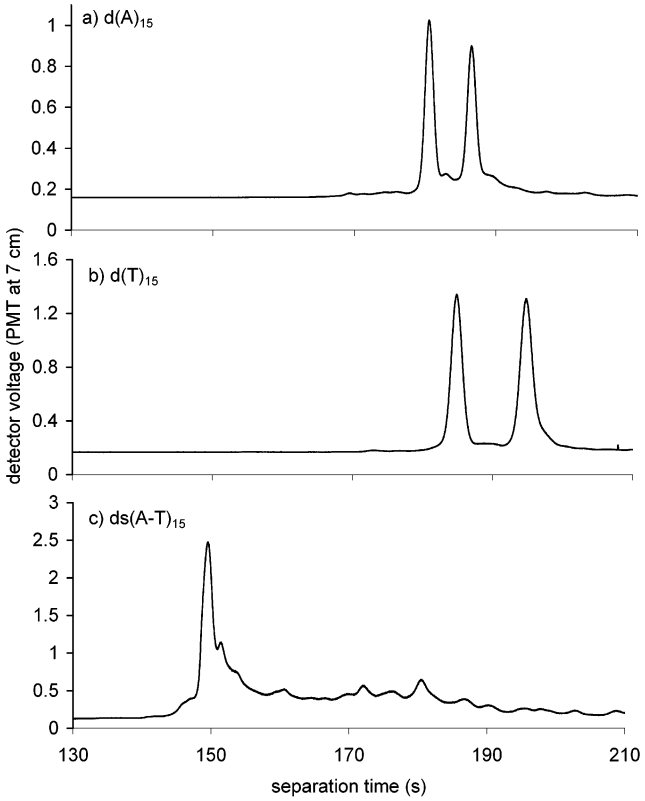

Figure 6. Free solution electrophoresis of Texas Red-labeled 15 mers: (a) $d(A)_{15}$, (b) $d(T)_{15}$, and (c) after the same two complement strands are hybridized in solution.

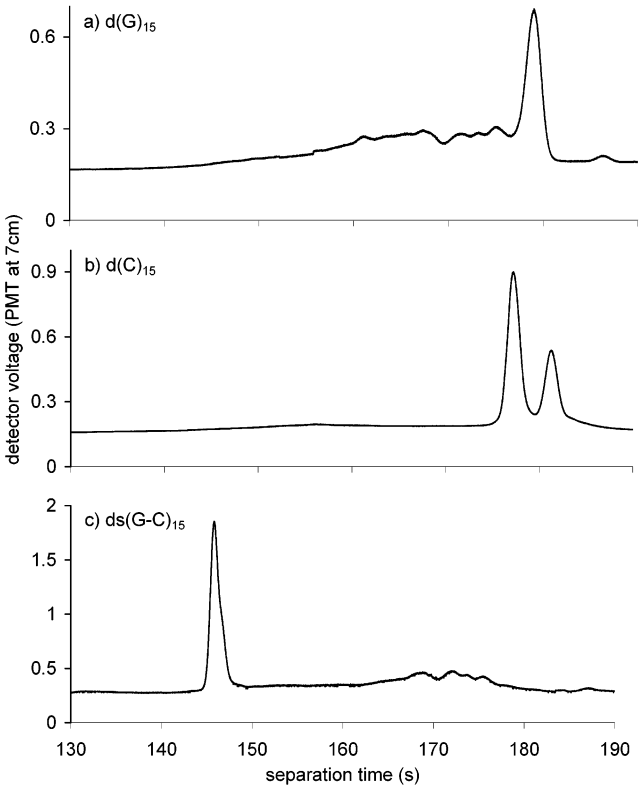

Figure 7. Free solution electrophoresis of Texas Red-labeled 15 mers: (a) $d(G)_{15}$, (b) $d(C)_{15}$, and (c) after the same two complement strands are hybridized in solution.

two peaks were observed for both $d(A)_{15}$ and $d(T)_{15}$ with the peaks for $d(T)_{15}$ migrating slightly slower than the peaks for $d(A)_{15}$. The mobility difference between these two sequences, which is 0.01×10^{-4} cm^2 V^{-1} s^{-1}, is within the 3% variance of our experimental measurements, making it impossible to determine whether mobility correlates to the base content. As for the other two oligomers, $d(C)_{15}$ and $d(G)_{15}$, panels a and b of Figure 7 show the electrophoresis of these oligomers at the same field strength of 588 V cm^{-1}.

The electrophoretic mobilities for these oligomers are also provided in Table 1. As with $d(T)_{15}$ and $d(A)_{15}$, there was also a slight difference in the mobilities between these two sequences, but again, these values are within the experimental variance of our measurements and cannot be used to infer a correlation between base content and mobility. However, a considerable difference in the peaks and the relative areas exists for each of the sequences. First, unlike poly d(T), poly d(A), and poly d(C), $d(G)_{15}$ appeared to contain a single band. Second, the relative peak areas for all four single-stranded oligomers varied with base content. Electrophoresis of ssDNA sequences containing single bases shows that the degree of band splitting is dependent upon the strand composition, suggesting a relationship between DNA structure and mobility.

If band splitting is indeed the result of different ssDNA structures, then a single band should be observed when these secondary structures are eliminated upon hybridization of complementary strands. Figures 6c and 7c show the electrophoresis of the $ds(T-A)_{15}$ and $ds(G-C)_{15}$ after allowing the ssDNA complementary strands to hybridize in the buffer for 30 min. Both electrophorograms contain a single major band at a retention time that corresponds to dsDNA; however, there is a considerable amount of tailing in this peak as well as a number of smaller peaks eluting at retention times greater than 165 s. A possible explanation for the presence of these additional peaks is that the Joule heating, as a result of the increased conductivity of the high buffer concentrations, is denaturing the dsDNA as it is migrating down the separation channel.

We therefore evaluated, both experimentally and theoretically, the increase in temperature due to Joule heating within the separation channel. By attaching a type T Teflon-insulated thermocouple to the bottom of the chip directly underneath and approximately halfway down the separation channel, a very gradual rise in temperature was measured over a time interval of 300 s, increasing ~2 °C above room temperature (24 °C). Using the measured electrical conductivity and current through the buffer, the power that transiently heats the chip was determined to be ~0.15 W, which is lost in the form of heat to the air surrounding the chip by natural convection. Based on the rate of Joule heating and by using the following correlation developed by Goldstein et al.,[32,33]

$$Nu = 0.54 Ra_L^{1/4}$$

the expected steady-state temperature was estimated to be 11 °C

(32) Goldstein, R. J.; Sparrow, E. W.; Jones, D. C. *Int. J. Heat Mass Transfer* **1973**, *16*, 1025−1035.

(33) Incropera, F. P.; DeWitt, D. P. *Fundamentals of Heat and Mass Transfer*, 5th ed.; John Wiley & Sons: New York, 2002; pp 545−557.

above room temperature. In this equation, where $Nu = hL/k$, h is the natural convection heat-transfer coefficient, k is the thermal conductivity of air, and the Rayleigh number is defined as

$$Ra_L = g\beta(T_s - T_\infty)L^3/\nu\alpha$$

where L is a characteristic length given by the surface area of the upper face of the chip divided by its perimeter, g is the acceleration due to gravity, β is the volumetric thermal expansion coefficient, which is the inverse of the temperature for an ideal gas, ν is the kinematic viscosity of air, and α is the thermal diffusivity of air. Note that this calculation assumes heat loss occurs from the upper surface only. This temperature, however, is not observed within the time of a typical experiment because one must also consider the time required to transfer heat within the chip. An estimate of this time is given by the square of the distance from the channel to the edge of the chip divided by the thermal diffusivity of the glass; a time of ~85 s after the start of the injection is required to begin heating the edges of the chip. Thus, heat is lost to the air in a region near the channel and the chip does not reach a constant temperature during a typical experiment. By adding a small desktop computer fan to convectively cool the chip, the steady-state temperature rise of ~1.2 °C is reached within 10−20 s. These temperature increases are consistent with the temperature rise seen in other chip-based capillary electrophoresis experiments and are in agreement with the anticipated steady-state temperature based on the flat-plate boundary layer correlation.[33−35]

$$Nu = 0.664Re^{1/2}Pr^{1/3}$$

where the Reynolds number, $Re = Uw/\nu$, U is the air velocity, w is the chip width of 1.6 cm, and $Pr = \nu/\alpha$. Since the dominant thermal resistance in dissipating the heat is from the surface of the chip to the surrounding air, the temperature of the chip and that in the fluid will be marginally higher, certainly less than 1 °C higher than the chip surface.[35]

Since the melting temperatures for these strands are greater than 50 (52 °C for ds(A−T) and 90 °C for ds(C−G)), the most reasonable explanation for the trailing peaks in Figures 6c and 7c, therefore, is the presence of staggered duplexes and multimers or aggregates, which are known to form when hybridizing complement strands with single-base content. Thermodynamic calculations based on the free energy changes for doublet formation were used to evaluate the formation of perfectly matched and staggered duplexes.[36,37] For $ds(A-T)_{15}$, the populations of perfectly matched, single-staggered (i.e., single-base dangling at each end), and a few multiply staggered hybrids have comparable melting temperatures (near 45 °C) while for $ds(G-C)_{15}$ even more staggered hybrids are expected to be stable at room temperature since the unstaggered hybrid has a melting temperature estimated to be ~98 °C. The tailing observed in the main peak as well as the numerous peaks detected after 165 s in Figures 6c and 7c are likely attributable to these staggered hybrids and multimers. However, comparable calculations on the random-sequence 15 mer of Figure 3 indicate that very little staggered hybrid should be present in this case at the near-room-temperature conditions used in this study. To confirm this, the random-sequence 15 mer of Figure 3 was hybridized to its complement strand and the resulting electrophorogram indeed exhibited very little tailing. The electrophorogram is presented in Supporting Information, and the data are consistent with the analysis that indicated less than 0.2% of the population would be staggered hybrids.

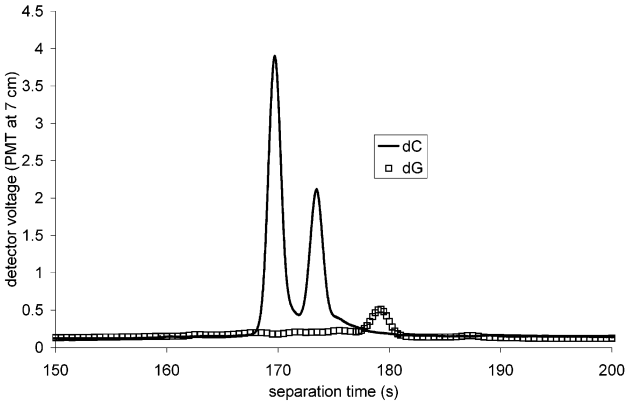

Figure 8. Overlay of the electrophoresis of $d(C)_{15}$ (—) and $d(G)_{15}$ (□) to evaluate quenching of Texas Red in the presence of guanine. Both measurements were performed with the same oligomer concentrations, 10.7 μM, and the same detector gain.

The measured electrophoretic mobilities for the each of dsDNA fragments are provided in Table 1. A comparison between the electrophoretic mobility of ssDNA to dsDNA indicates that ssDNA migrates ~12% slower than dsDNA. This is consistent with previous experiments where the mobilities of single-stranded DNA were determined to be ~15% lower than their double-stranded counterparts.[38,39]

One other very significant and noticeable difference in the electrophoresis of the ssDNA fragments is a significant decrease in the fluorescence emission from the Texas Red-labeled $d(G)_{15}$ when compared to the other three sequences analyzed. To illustrate this, Figure 8 shows an overlaid electrophorogram containing equal concentrations of $d(C)_{15}$ and $d(G)_{15}$ obtained with the same PMT gain.

This decrease in fluorescence suggests quenching of the fluorescent label, Texas Red, in the presence of guanine. In fact, recent fluorescence lifetime studies have shown that guanine does quench a number of fluorophores including Texas Red.[40−45] These studies confirmed the existence of a ground-state complex that

(34) Knox, J. H.; McCormack, K. A. *Chromatographia* **1994**, *38*, 207−214.
(35) Swinney, K.; Bornhop, D. J. *Electrophoresis* **2002**, *23*, 613−620.
(36) SantaLucia, J., Jr.; Allawi, H. T.; Seneviratne, P. A. *Biochemistry* **1996**, 3555−3562.
(37) Bommarito, S., Peyret, N., SantaLucia, J., Jr. *Nucleic Acids Res.* **2000**, *28*, 1929−1934.
(38) Constatino, L.; Liquori, A. M. *Biopolymers* **1964**, *2*, 1−8.
(39) Olivera, B. M.; Baine, P.; Davidson, N. *Biopolymers* **1964**, *2*, 245−257.
(40) Seidel, C. A. M.; Schulz, A.; Sauer, M. H. M. *J. Phys. Chem.* **1996**, *100*, 5541−5553.
(41) Edman, L.; Mets, U.; Rigler, R. *Proc. Natl. Acad. Sci. U.S.A.* **1996**, *93*, 6710−6715.
(42) Sauer, M.; Drexhage, K. H.; Lieberwirth, U.; Muller, R.; Nord, S.; Zander, C. *Chem. Phys. Lett.* **1998**, *284*, 153−163.
(43) Eggeling, C.; Fries, J. R.; Brand, L.; Gunther, R.; Seidel, C. A. M. *Proc. Natl. Acad. Sci. U.S.A.* **1998**, *95*, 1556−1561.
(44) Knemeyer, J.-P.; Marme, N.; Sauer, M. *Anal. Chem.* **2000**, *72*, 3717−3724.
(45) Torimura, M.; Shinya, K.; Yamada, K.; Yokomaku, T.; Kamagata, Y.; Kanagawa, T.; Kurane, R. *Anal. Sci.* **2001**, *17*, 155−160.

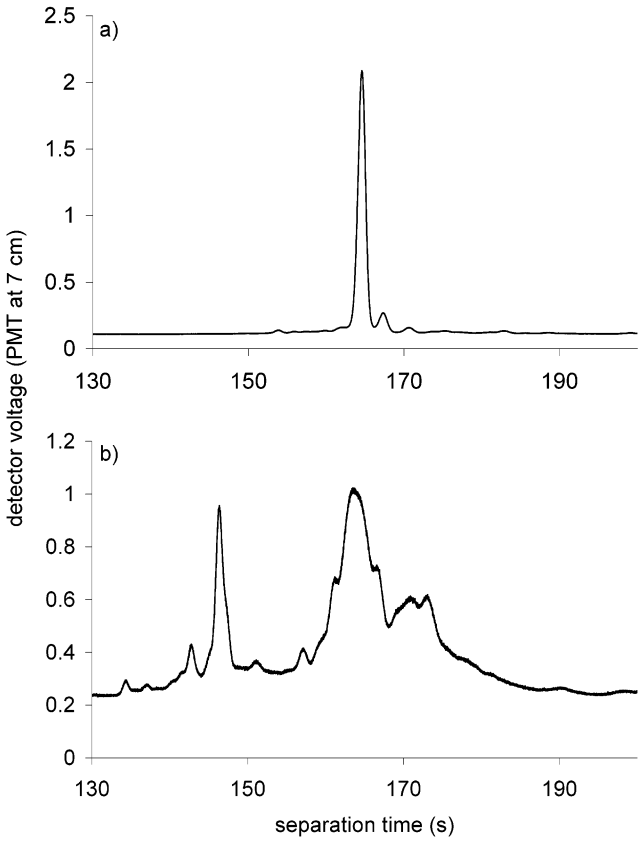

Figure 9. Free solution electrophoresis of Cy3-labeled 15 mers: (a) $d(A)_{15}$ and (b) $d(G)_{15}$.

forms as a result of a hydrophobic interaction between the fluorescent dye and individual nucleotide bases in polar solvents. This complex, when formed in the presence of guanine, allows the transfer of an electron from the ground state of guanine to the excited state of the fluorescent dye, leading to the quenching.[40,45] Therefore, for us to observe this quenching during electrophoretic migration, the dye must be interacting with the guanine bases in the strand instead of tailing behind like a ball at the end of a string, which is the assumed structure in ELFSE.

To confirm that the multiple peaks observed for ssDNA are attributable to hydrophobic interactions between the dye and nucleotide bases, the fluorescent label on two of the four oligomers was changed to Cy3, a negatively charged fluorescent label that has been shown not to be quenched by guanine.[45] Figure 9 shows electrophorograms for $d(A)_{15}$ and $d(G)_{15}$ that are labeled with Cy3 at the 5′ end.

As Figure 9a shows, the electrophorogram for $d(A)_{15}$ only has one major peak with two smaller peaks while the electrophorogram for $d(G)_{15}$ in Figure 9b contains a multitude of peaks that elute from 135 to 180 s. Both of these results show that changing the fluorescent label influences the number of conformations that are present during electrophoresis and confirms an interaction between the dye and the bases within ssDNA. One key unresolved issue is why the fluorescent-labeled $d(G)_{15}$ exhibits multiple peaks. Recent studies into the structure of telomeres have shown that oligomers containing multi-guanine tracks can form a multitude of secondary structures from non-Watson and Crick or Hoogstein base pairing.[46−52] Such bonding can result in intrastrand and interstrand G-quadruplex structures.[51] Therefore, the peaks that elute around the same time as dsDNA (135−155 s) are most likely interstrand G-quadruplexes while those that elute around the same times as ssDNA (>155 s) are most likely intrastrand G-quadruplexes. This is the first time free solution electrophoresis has been used to observe secondary structures of telomere-like ssDNA.

CONCLUSIONS

By using a high buffer (10× TBE) concentration, electroosmotic flow within uncoated glass channels was minimized enough to allow for the free solution electrophoresis of both ssDNA and dsDNA. Under standard capillary electrophoresis conditions, such buffers would result in a significant amount of Joule heating; however, since the geometric dimensions of the microfluidic chip channels result in a higher surface-to-volume ratio than standard circular capillaries, efficient heat dissipation limited the temperature increase to 2 °C during our longest separation time (350 s) and at the highest field applied (∼600 V cm^{-1}). These higher field strengths significantly increased the electrophoretic velocities and in turn decreased the separation times. As a result, molecular diffusion was minimized, facilitating the separation of ssDNA fragments containing a random sequence of 21, 15, and 9 bases in length within a separation length of 4 cm. Unexpectedly, each single-stranded oligomer exhibited two well-resolved peaks at these higher field strengths. As this investigation shows, the number of peaks and relative areas varied as a function of base content and fluorescent label, Texas Red versus Cy3. These changes, along with the observed quenching of Texas Red by the nucleotide base guanine, confirmed that these multiple peaks correspond to different secondary structures associated with hydrophobic interactions between the nucleotide bases of ssDNA and the fluorescent dye, Texas Red. The results of this investigation improve our understanding of the relationship between free solution electrophoretic mobility and the composition of small DNA oligomers.

ACKNOWLEDGMENT

This work was supported by the W. M. Keck Foundation and a NIH K25 Award (J.D.S.). We thank Dr. Robert Doebler for assistance with temperature measurements on the microfluidic chip and Professor Greg Dewey for his assistance with the theoretical calculations of duplex melting temperatures.

SUPPORTING INFORMATION AVAILABLE

Results of the polarity switching experiment and the 15-bp duplex study to determine the prevalence of staggered multimers. This material is available free of charge via the Internet at http://pubs.acs.org/ac.

Received for review March 31, 2003. Accepted July 14, 2003.

AC034326C

(46) Sen, D.; Gilbert, W. *Biochemistry* **1992**, *31*, 65−70.
(47) Venczel, E. A.; Sen, D. *Biochemistry* **1993**, *32*, 6220−6228.
(48) Miura, T.; Thomas, G. J., Jr. *Biochemistry* **1995**, *34*, 9645−9654.
(49) Protozanova, E.; Macgregor, R. B., Jr. *Biochemistry* **1996**, *35*, 16638−16645.
(50) Protozanova, E.; Macgregor, R. B., Jr. *Biophys. Chem*. **1998**, *75*, 249−257.
(51) Poon, K.; Macgregor, R. B., Jr. *Biopolymers* **1998**, *45*, 427−434.
(52) Kypr, J.; Vorlickova, M. *Biopolymers (Biospectroscopy)* **2002**, *67*, 275−277.